J Supercond Nov Magn (2013) 26:719–723
DOI 10.1007/s10948-012-1798-4

ORIGINAL PAPER

Studies on Low-Field and Room-Temperature Magnetoresistance in $La_{2/3}(Ca_{1-x}Sr_x)_{1/3}MnO_3$ Perovskites

D.G. Li · Y.T. Mai · J. Xoing · Y.H. Xiong · Z.L. Liu · C.S. Xiong

Received: 13 July 2012 / Accepted: 14 November 2012 / Published online: 12 December 2012

Abstract The polycrystalline perovskites $La_{2/3}(Ca_{1-x}Sr_x)_{1/3}MnO_3$ ($x = 0, 0.2, 0.4, 0.6, 0.8, 1$) were successfully prepared by a modified method of solid-state reactions, in which the ingredient mixture with ethanol as a liquid milling medium to form suspension was milled by high-energy ball milling for 10 h and sintered in air at 1400 °C for 10 h. The microstructure, electrical transport, and low-field magnetoresistance (LFMR) of the perovskites were investigated to study the room-temperature magnetoresistance (RTMR) behavior. The results reveal that the metal-to-insulator transition temperature (T_{MI}) increased with increasing doping level x, and the peak values of the magnetoresistance (MR) near T_{MI} dropped with the more Ca^{2+} substituted. A single-phase $La_{2/3}Ca_{1/3}MnO_3$ showed T_{MI} at 263 K and the peak MR of 23 % in the applied field of 3 kOe near T_{MI}. The LFMR effect at room temperature could be obtained by controlling the doping Sr^{2+}-substituted Ca^{2+} level. When $x = 0.29$, transition temperature (T_{MI}) was 305.30 K, and the MR effect was recorded up to 12.9 % at 298.55 K and 3 kOe. Finally, the possible mechanism is discussed.

Keywords Magnetoresistance · Manganite · Polycrystalline perovskite · High-energy ball milling · Low-field magnetoresistance

D.G. Li · Y.T. Mai · Y.H. Xiong · Z.L. Liu · C.S. Xiong (✉)
Department of Physics, Huazhong University of Science and Technology, Wuhan 430074, P.R. China
e-mail: csxiong@mail.hust.edu.cn

D.G. Li · J. Xoing
College of Science, Naval University of Engineering, Wuhan 430033, P.R. China

1 Introduction

Intense researches have been carried out for the potential application of magnetic field sensor and magnetic recording, since large magnetoresistance (MR) effect was discovered in the doped manganese oxide $Re_{1-x}A_xMnO_3$ (Re = trivalent rare earth and A = divalent metal). This kind of perovskite possesses unique properties as the colossal magnetoresistance (CMR), metal-to-insulator (M-I) transition and phase separation, etc. The Double Exchange (DE) mechanism was first put forward to explain the electron transport property [1, 2]. Later researches on the phase diagram [3], oxygen influence [4, 5], charge ordering [6], Jahn–Teller effect [7, 8], and grain boundary and lattice effect [9–11] have made contribution to understanding the mechanism of the doped rare earth manganese perovskite. The CMR usually occurs at low temperature range and strong magnetic field, and this has become the main obstacle to the practical application. Nowadays, researchers are focusing on how to obtain a large value of the MR at a low field and room temperature in order to satisfy practical applications. The LFMR [12–15], which is the significant MR effect that can be observed at a low magnetic field just several thousand mT or below, has been triggered renewal researches on the polycrystalline doped rare earth manganese perovskite. The LFMR is usually observed at low temperature and believed to be aroused by the spin-dependent scattering [16, 17] or spin-dependent tunneling [18–20] on the grain boundaries. The transport property is sensitive to the characteristics of grain boundaries, so samples with smaller grain will exhibit larger LFMR. This recalls people to restudy the synthesis of manganese perovskite.

As we know, the magnetic-ordering temperature T_C of $La_{1-x}Ca_xMnO_3$ (LCMO) is below room temperature at about 270 K [21], while T_C of $La_{1-x}Sr_xMnO_3$ (LSMO) is

far above the room temperature, and the highest temperature is about 360 K [22]. At the transition temperature, the MR value of LCMO is relatively greater than that of LSMO. The nature of ferromagnetic phase transition and its critical properties in $La_{0.7}Ca_{0.3-x}Sr_xMnO_3$ ($x = 0, 0.05, 0.1, 0.2$, and 0.25) single crystals have been studied systematically by Phana et al. [23]. So we can change the value of x in $La_{2/3}(Ca_{1-x}Sr_x)_{1/3}MnO_3$ to systematically study the room-temperature MR effect.

In this paper, we have employed high-energy ball milling to refine the ingredient mixture by adding ethanol as a liquid milling medium to form suspension before milling and heat treatment [24]. This method is different from the traditional mechanical alloying [25, 26] and mechanochemical processing [27], and we only intend to reduce the size of the particles by ball milling but not any amorphization or chemical reactions [28]. Ethanol can absorb some of the heat that is generated due to the milling process, as well as separate the new formed surface of ground powders to avoid recombination or reactions. Simultaneously, powders can suffer more profound milling, which was helpful for obtaining the smaller particle size and avoiding the inhomogeneity to be introduced. By this method, the polycrystalline perovskites $La_{2/3}(Ca_{1-x}Sr_x)_{1/3}MnO_3$ (LCSMO) ($x = 0, 0.2, 0.4, 0.6, 0.8, 1$) were successfully synthesized. The microstructure and transportation of LCSMO have been investigated. We have also discussed the relation between the peak MR value, the metal-to-insulator transition temperature (T_{MI}), and doped level of x.

2 Experimental

Stoichiometric amount of commercial $La(OH)_3$, $CaCO_3$, $SrCO_3$, and MnO_2 powders were mixed according to formula $La_{2/3}(Ca_{1-x}Sr_x)_{1/3}MnO_3$ ($x = 0, 0.2, 0.4, 0.6, 0.8, 1$) with ethanol and milled by a planetary ball miller. The milling time (t_m) was set to be 10 h. The as-milled powders were dried at 90 °C and pressed into pieces, followed by sintering process at 1400 °C for 10 h in air [24].

Both of the as-milled powder and the ceramic samples were characterized by X-ray diffraction (XRD) to confirm the crystalline phase. Scanning electron microscopy (SEM) was employed to examine the microstructure of samples. The electrical and magnetic transport behaviors were measured by the standard dc four-probe method in the temperature range from 50 to 400 K at an external field of 3 kOe.

3 Results and Discussions

Figure 1 shows the XRD patterns of the starting materials and the as-milled powders. The average diameter of as-milled powder was about 90 nm by the classical Sheerer formula calculation. Since no new diffraction peaks came up,

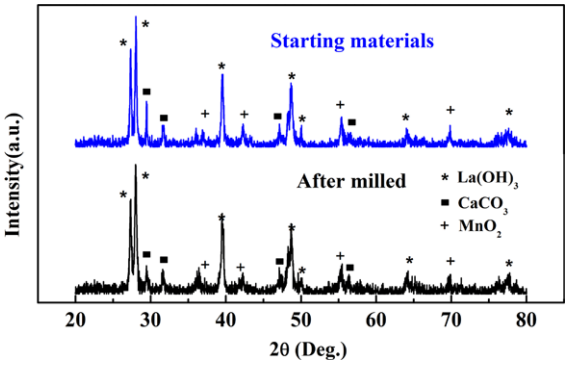

Fig. 1 XRD patterns of starting powders and as-milled powders for milling time of 10 hours. The *asterisk symbol* denotes the $La(OH)_3$; *solid square* denotes $CaCO_3$; *cross* stands for MnO_2

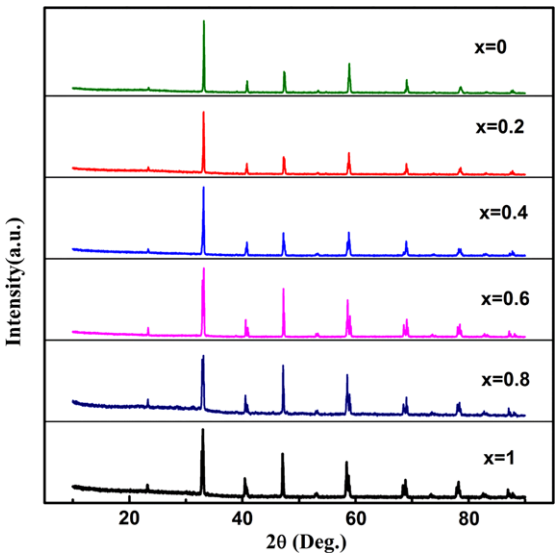

Fig. 2 XRD patterns of heat treated samples. All samples showed the characteristic peaks of the pseudo-cubic perovskite structure

it could be seen that not any amorphization or chemical reactions occurred, and the as-milled powders still remained in their starting composition. The improved ball milling method with ethanol as a liquid ingredient mixture medium to form suspension is helpful for reducing particle size and obtaining homogeneous powders.

From Fig. 2 we can see that all of the heat treated samples have crystallized into single-phase perovskites, and this means that the doped lanthanum manganese perovskites have been successfully synthesized by this modified method.

Figure 3 displays the SEM result of $La_{2/3}Ca_{1/3}MnO_3$. The morphology of this ceramic was identical with those synthesized by solid-state reaction. We can find out that the well-crystallized grain sizes of the ceramics were uniformly in the range of 4–5 μm.

Magnetoresistance of investigated ceramic samples was measured as a function of temperature and magnetic field. Here MR was defined as MR (%) $= [-(\rho_H - \rho_0)/\rho_0] \times$

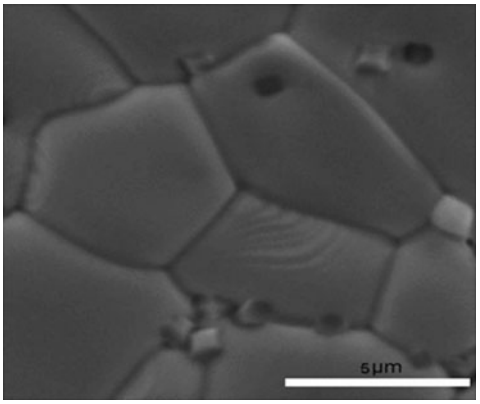

Fig. 3 Typical SEM image for $La_{2/3}Ca_{1/3}MnO_3$ ($x = 0$) ceramic. The average grain size was in the range of 4–5 μm

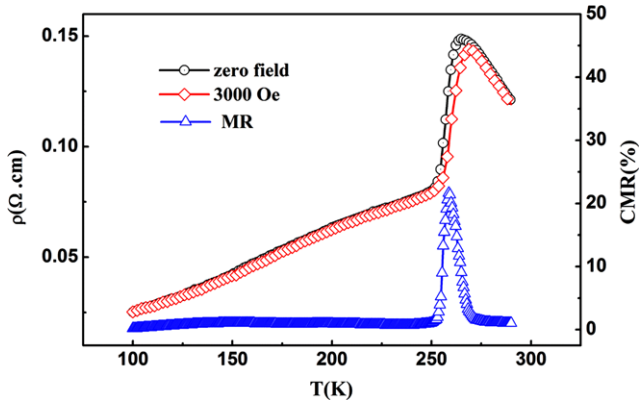

Fig. 4 Transport properties of $La_{2/3}Ca_{1/3}MnO_3$ ($x = 0$) ceramic

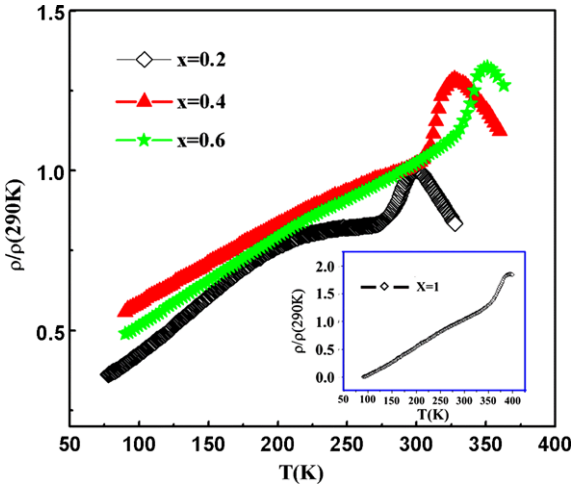

Fig. 5 Transport properties of $La_{2/3}(Ca_{1-x}Sr_x)_{1/3}MnO_3$ for $x = 0.2$, 0.4, 0.6 and 1

100 %, where ρ_0 and ρ_H are the resistivity in applied magnetic field of zero and 3 kOe, respectively. The temperature-dependent transportation of $La_{2/3}Ca_{1/3}MnO_3$ is shown in Fig. 4. The transition temperature (T_{MI}) was 265.08 K, and

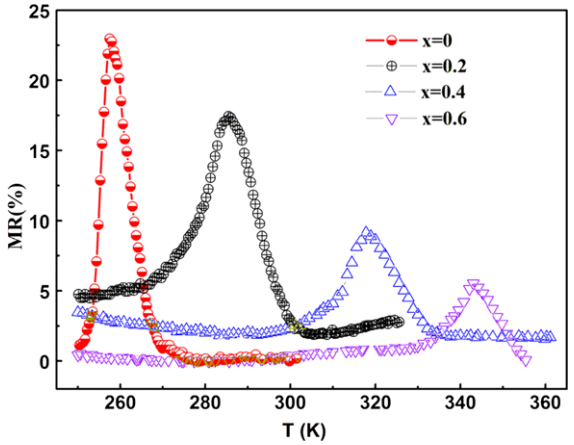

Fig. 6 Peak MR values near T_{MI} of $La_{2/3}(Ca_{1-x}Sr_x)_{1/3}MnO_3$ for $x = 0$, 0.2, 0.4 and 0.6 at 3 kOe

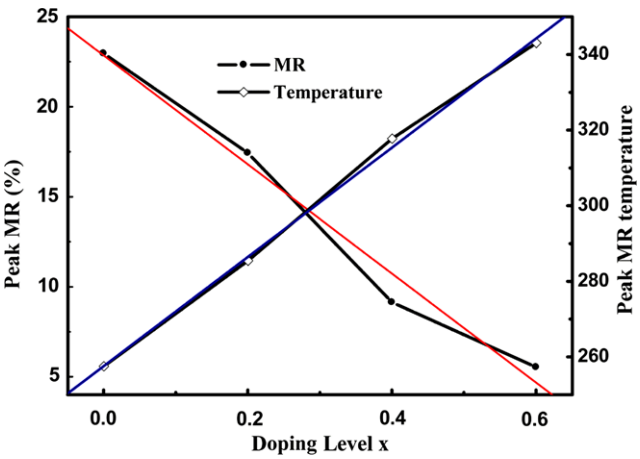

Fig. 7 The peak MR values/peak MR temperatures versus

the peak MR was recorded up to 22.96 % at 257.51 K. The resistivity-versus-temperature and MR curves for LCSMO samples are shown clearly for different doping levels in Fig. 5 and Fig. 6. When Ca^{2+} was substituted by Sr^{2+}, increase of T_{MI} kept continuing as the doping level x of Sr increased. The changes of transition temperatures were shown clearly for different doping levels. T_{MI} of samples with varied Sr concentrations all jumped above room temperature. The exact values are 289.71 K, 327.45 K, 352.05 K, and 393.23 K for the samples with $x = 0.2$, 0.4, 0.6, and 1, respectively. Meanwhile, the peak MR values near T_{MI} versus doping level different changed. The more Ca was substituted by Sr, the less peak MR amplitude became. For $x = 0.2$, 0.4, and 0.6, the maximum MR values were 17.26 %, 9.05 %, and 5.42 % at 3 kOe, and the corresponding transition temperatures were 285.41 K, 317.84 K, and 342.90 K, respectively.

In Fig. 7, the peak MR values and peak MR temperatures versus the doping level x are shown. It was shown that Ca^{2+} substituted by Sr^{2+} has a great impact on trans-

Table 1 Refined cell parameters obtained for the $La_{2/3}(Ca_{1-x}Sr_x)_{1/3}MnO_3$ compounds

Sample	$x = 0$	$x = 0.2$	$x = 0.4$	$x = 0.6$	$x = 0.8$	$x = 1$
Space group	Pnma	Pnma	Pnma	Pc/2	Pc/2	Pc/2
Structure type	Orthorhombic	Orthorhombic	Orthorhombic	Monoclinic	Monoclinic	Monoclinic
a (Å)	5.4347	5.4401	5.4412	5.4123	5.4245	5.4218
b (Å)	5.4623	5.4583	5.4731	5.4826	5.4892	5.4869
c (Å)	7.6729	7.6742	7.6446	7.6952	7.7065	7.7306
V (Å^3)	227.78	227.88	227.66	228.34	229.47	229.98

port properties of LCSMO. We can find out that the temperature at which peak MR occur is almost proportional to the amount of Sr doping level, while the peak MR is nearly inverse-proportional to x. So we can deduce that an MR of 13.5 % can be obtained at room temperature of 300 K with amount of Sr doping level for $x = 0.29$. So $La_{2/3}(Ca_{1-x}Sr_x)_{1/3}MnO_3$ with $x = 0.29$ was successfully synthesized by the above same synthesis method, followed by studies on the RTMR behavior. The results have shown that T_{MI} was 305.30 K, and the MR effect was recorded up to 12.9 % at 298.55 K.

These results show that we can balance the peak MR values and the peak MR temperature by controlling the doping level x of A site cation for $Re_{1-x}A_xMnO_3$. Generally, the MR near T_{MI} is closely related to the Double Exchange (DE) mechanism. With the same other conditions, small average A site ion radius leads to lower T_C and larger MR near T_{MI}. A site doping cations (A^{2+}) do not participate in the DE interaction but show influence through coupling with B site (Mn) cations, and finally alter the Curie temperature (T_C) and MR decreases. Considering a substitution of A site cations by ions with different lattice energy, it is expected that a ceramic with transition temperature and significant MR value in room temperature range and low magnetic field is possible. Since Sr^{2+} has a larger cation radius than that of Ca^{2+}, when concentration of Sr^{2+} become larger, the bond angle and bond length of Mn–O–Mn pairs are changed and lead to T_{MI} raised and peak MR value near T_{MI} dropped. In our case, even when Ca^{2+} is gradually substituted by Sr^{2+}, since both ions are of the same valence, the Mn^{3+}/Mn^{4+} is not changed. But the radius of Sr^{2+} is larger than Ca^{2+}, therefore the average A site cation radius is increased, and then T_C (related to T_{MI}) shifts to higher temperature while peak MR near T_{MI} drops. We can obtain the significant MR value in room temperature range and low magnetic field to satisfy practical applications by controlling the doping level x of Sr for LCSMO.

On the other hand, the results also showed a jump at $x = 0.4$ in Fig. 7. So we have further processed the XRD data in Fig. 2, the crystallite sizes were refined by Rietveld refinement technique, and the cell parameters of all the samples are listed in Table 1. It should be noticed the lattice parameters increase with Sr content. The LCSMO compounds have undergone a structural orthorhombic-to-monoclinic transition during the variation of x from 0.4 to 0.6. These results are similar to the observation obtained by Brankovic et al. [23], in which they have reported that with increasing values of dopant radius ($Ca^{2+} < Sr^{2+}$) transition temperature tend to be shifted to higher temperature and decreased the magnetoresistance. A systematic investigation by Thanh et al. [29, 30] for the ferromagnetic phase transitions and critical behavior of $La_{0.7}Ca_{0.3-x}Sr_xMnO_3$ ($x = 0, 0.05, 0.1, 0.2$, and 0.25) single crystals also showed the structure changes during the variation of x, and it was at $x = 0.15$. This can explain the reason of the jump at $x = 0.4$ in Fig. 7.

4 Conclusions

Nanocrystalline $La_{2/3}(Ca_{1-x}Sr_x)_{1/3}MnO_3$ materials were successfully synthesized by an improved high-energy ball milling with ethanol as a liquid medium and post sintering method. We have studied the microstructure, electrical transport and low-field MR effect by changing the value of x in $La_{2/3}(Ca_{1-x}Sr_x)_{1/3}MnO_3$. The results showed that T_{MI} increased with increasing doping level x. On the contrary, the peak MR values near T_{MI} dropped with the more Ca^{2+} substituted. And we deduced that the low-field MR effect at room temperature could be obtained by controlling the doping Sr^{2+} substituted Ca^{2+} level. In $La_{2/3}(Ca_{1-x}Sr_x)_{1/3}MnO_3$ with $x = 0.29$, T_{MI} was 305.30 K, and the MR effect was recorded up to 12.9 % at 298.55 K and 3 kOe.

Acknowledgements This work was supported by the National Science Foundation of China (Grant No. 20971048). The authors thank Analytical and Testing Center of Huazhong University of Science and Technology, which supplied us the facilities to fulfill the measurement.

References

1. Zener, C.: Phys. Rev. **82**, 403 (1951)
2. Anderson, P.W., Hasegawa, H.: Phys. Rev. **100**, 675 (1955)
3. Schiffer, P., Ramirez, A.P., Bao, W., Cheong, S.W.: Phys. Rev. Lett. **75**, 3336 (1995)
4. Sun, J.R., Rao, G.H., Zhang, Y.Z.: Appl. Phys. Lett. **72**, 3208 (1998)
5. Akther Hossain, A.K.M., Cohen, L.F., Kodenkandeth, T., MacManus-Driscoll, J., McN. Alford, N.: J. Magn. Magn. Mater. **195**, 31 (1999)
6. Mori, S., Chen, C.H., Cheong, S.W.: Nature (London) **392**, 473 (1998)
7. Millis, A.J., Littlewood, P.B., Shraiman, B.I.: Phys. Rev. Lett. **74**, 5144 (1995)
8. Zheng, R.K., Li, G., Tang, A.N., Yang, Y., Wang, W., Li, X.G., Wang, Z.D., Ku, H.C.: Appl. Phys. Lett. **83**, 5250 (2003)
9. Terai, T., Murata, T., Fukuda, T., Kakeshita, T.: J. Phys. Condens. Matter **16**, 5801 (2004)
10. Gupta, A., Gong, G.Q., Xiao, G., Duncombe, P.R., Lecoeur, P., Trouilloud, P., Wang, Y.Y., Dravid, V.P., Sun, J.Z.: Phys. Rev. B **54**, 629 (1996)
11. Hwang, H.Y., Cheong, S.W., Radaelli, P.G., Marezio, M., Batlogg, B.: Phys. Rev. Lett. **75**, 914 (1995)
12. de Andres, A., Taboada, S., Colino, J.M., Ramirez, R., Garcia-Hernandez, M., Martinez, J.L.: Appl. Phys. Lett. **81**, 319 (2002)
13. Shlyakhtin, O.A., Shin, K.H., Oh, Y.J.: J. Appl. Phys. **91**, 7403 (2002)
14. Huang, B.X., Liu, Y.H., Zhang, R.Z., Xiao, B.Y., Wang, C.J., Mei, L.M.: J. Phys. D **36**, 1923 (2003)
15. Wang, T., Chen, X.M., Wang, F.F., Shi, W.Z.: Physica B **405**, 3088 (2010)
16. Gupta, A., Sun, J.Z.: J. Magn. Magn. Mater. **200**, 24 (1999)
17. Li, X.W., Gupta, A., Xiao, G., Gong, G.Q.: Appl. Phys. Lett. **71**, 1124 (1997)
18. Hwang, H.Y., Cheong, S.W., Ong, N.P., Batlogg, B.: Phys. Rev. Lett. **77**, 2041 (1996)
19. Wang, Z.H., Ji, T.H., Wang, Y.Q., Chen, X., Li, R.W., Cai, J.W., Sun, J.R., Shen, B.G., Yan, C.H.: J. Appl. Phys. **87**, 5582 (2000)
20. Siwach, P.K., Singh, H.K., Srivastava, O.N.: J. Phys. Condens. Matter **20**, 273 (2008)
21. Gaur, A., Varma, G.D.: J. Alloys Compd. **453**, 423 (2008)
22. Mikhaleva, E.V., Vasil'ev, V.G., Nosov, A.P., Vladimirova, E.V., Slobodin, B.V.: Phys. Chem. Glasses **35**, 81 (2009)
23. Brankovic, Z., Đuris, K., Radojkovic, A., Bernik, S., Jaglicic, Z., Jagodic, M., Vojisavljevic, K., Brankovic, G.: J. Sol-Gel Sci. Technol. **55**, 311 (2010)
24. Xiong, C.S., Mai, Y.T., Xiong, Y.H., Pi, H.L., Ren, Z.M., Zhang, J., Pi, Y.B., Xu, W., Dai, G.H., Song, S.J., Yang, S.: Mater. Res. Bull. **42**, 904 (2007)
25. Jin, Z.Q., Tang, W., Zhang, J.R., Du, Y.W.: J. Magn. Magn. Mater. **187**, 237 (1998)
26. Muroi, M., Street, R., McCormick, P.G.: J. Solid State Chem. **152**, 503 (2000)
27. Muroi, M., Street, R., McCormick, P.G.: J. Appl. Phys. **87**, 3424 (2000)
28. Suryanarayana, C.: Prog. Mater. Sci. **46**, 1 (2001)
29. Thanh, T.D., Nguyen, L.H., Manh, D.H., Chien, N.V., Phong, P.T., Khiem, N.V., Hong, L.V., Phuc, N.X.: Physica B **407**, 145 (2012)
30. Phan, M.H., Franco, V., Bingham, N.S., Srikanth, H., Hur, N.H., Yu, S.C.: J. Alloys Compd. **508**, 238 (2010)